

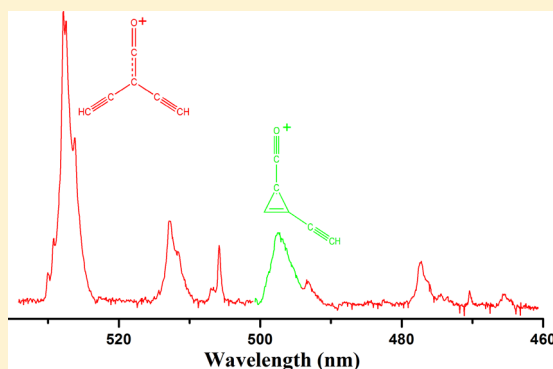
# Electronic Absorption Spectra of $\text{H}_2\text{C}_6\text{O}^+$ Isomers: Produced by Ion–Molecule Reactions

Arghya Chakraborty, Jan Fulara, and John P. Maier\*

Department of Chemistry, University of Basel, Klingelbergstrasse 80, CH-4056, Basel, Switzerland

## S Supporting Information

**ABSTRACT:** Three absorption systems with origins at 354, 497, and 528 nm were detected after mass-selected deposition of  $\text{H}_2\text{C}_6\text{O}^+$  in a 6 K neon matrix. The ions were formed by the reaction of  $\text{C}_2\text{O}$  with  $\text{HC}_4\text{H}^+$  in a mixture of  $\text{C}_3\text{O}_2$  and diacetylene in a hot cathode source, or by dissociative ionization of tetrabromocyclohexadienone. The 497 and 354 nm systems are assigned to the  $1^2\text{A}'' \leftarrow \text{X}^2\text{A}''$  and  $2^2\text{A}'' \leftarrow \text{X}^2\text{A}''$  electronic transitions of  $\text{B}^+$ , (2-ethynylcycloallyl)methanone cation, and the 528 nm absorption to the  $1^2\text{A}_2 \leftarrow \text{X}^2\text{B}_1$  transition of  $\text{F}^+$ , 2-ethynylbut-3-yn-1-enone-1-ylide, on the basis of calculated excitation energies with CASPT2.



## 1. INTRODUCTION

Production of oxygenated hydrocarbons in interstellar clouds is a challenging issue in astrochemical research. Though oxygen has a cosmic abundance similar to carbon, the number of oxo-organic species detected in interstellar and protostellar regions is smaller than the number of hydrocarbons.<sup>1–4</sup> One reason is that oxygen is locked up in the oxides of carbon, silicon, and refractory metals, and CO is the most abundant molecule, after  $\text{H}_2$ , in space.<sup>5–10</sup>

One of the ways to produce oxygen containing species in the interstellar medium (ISM) is radiative association of atomic oxygen with hydrocarbons.<sup>2</sup> An example of this could be cyclopropenone ( $\text{c-H}_2\text{C}_3\text{O}$ ), which has been detected in Sagittarius B2(N),<sup>11</sup> a region where cyclopropenylidene ( $\text{c-C}_3\text{H}_2$ ) has also been observed. Recently, the larger abundance of long chain hydrocarbon anions in denser clouds has been attributed to the depletion of oxygen atoms. Postulated reaction models suggest that these anions react with oxygen atoms and form oxygenated hydrocarbon and carbon oxides.<sup>12</sup> Carbon monoxide is also taken into account for the formation of oxygenated species in the ISM via radiative association reactions.<sup>13</sup>

In this context, reactions of some astrochemically relevant ions as  $\text{C}_4\text{H}^+$ ,  $\text{C}_4\text{H}_2^+$ ,  $\text{C}_4\text{H}_3^+$ ,  $\text{C}_5\text{H}^+$ , and  $\text{C}_6\text{H}^+$  with CO and  $\text{O}_2$  were studied by the selected-ion flow tube technique. All of these species reacted with CO, giving monooxygenated hydrocarbon cations.<sup>13</sup>  $\text{HCO}^+$ ,  $\text{HCO}_2^+$ , and  $\text{H}_3\text{CO}^+$  are the only three oxygen containing hydrocarbon cations detected so far in the ISM by radioastronomy.<sup>14–17</sup> In the laboratory,  $\text{HC}_n\text{O}$  ( $n = 1–7$ ) were studied by microwave spectroscopy.<sup>18–22</sup> A few oxides of carbon chains were studied in rare gas matrixes as well,<sup>23,24</sup> but spectroscopy of oxygenated hydrocarbon cations is unknown.

In this contribution the electronic absorption spectra of  $\text{H}_2\text{C}_6\text{O}^+$  trapped in 6 K neon matrixes are presented and assigned to two isomers on the basis of calculated excitation energies using the CASPT2 method. These species are formed via a reaction of  $\text{C}_2\text{O}$  with hydrocarbon cations in the discharge source.

## 2. EXPERIMENTAL SECTION

**2.1. Production of Ions.** A 1:1 mixture of carbon suboxide and diacetylene diluted with helium was used to produce  $\text{H}_2\text{C}_6\text{O}^+$  in a hot discharge source. Pure  $\text{C}_3\text{O}_2$  or  $\text{HC}_4\text{H}$  does not yield the  $m/z = 90$  peak in the mass spectrum, but it appears in their mixture (Figure 1, green trace). The  $\text{C}_2\text{O}^+$  and  $\text{CO}^+$  fragment ions are present in the mass spectrum of  $\text{C}_3\text{O}_2$  (Figure 1, red) and in the mixture with  $\text{HC}_4\text{H}$ .  $\text{H}_2\text{C}_6\text{O}^+$  can be formed in the source by insertion of the  $\text{C}_2\text{O}^+$  fragment into  $\text{HC}_4\text{H}$  or  $\text{C}_2\text{O}$  into  $\text{HC}_4\text{H}^+$ . As  $\text{HC}_6\text{H}^+$  is present in the mass spectrum of diacetylene, as well as in the mixture with carbon suboxide, formation of  $\text{H}_2\text{C}_6\text{O}^+$  could also proceed via reaction of  $\text{CO}/\text{CO}^+$  with  $\text{HC}_6\text{H}^+/\text{HC}_6\text{H}$ . However, this is excluded because the  $m/z = 90$  cation was not observed with a  $\text{CO}/\text{HC}_4\text{H}$  mixture under similar conditions whereas the mass peak of  $\text{HC}_6\text{H}^+$  was intense. It was found that the intensity of the  $\text{C}_2\text{O}^+$  and  $\text{H}_2\text{C}_6\text{O}^+$  ions produced under different discharge conditions are correlated, suggesting that the formation of  $\text{H}_2\text{C}_6\text{O}^+$  depends on the production of  $\text{C}_2\text{O}^+$ .  $\text{H}_2\text{C}_6\text{O}^+$  was also produced from a vapor of 2,4,4,6-tetrabromo-2,5-cyclohexadienone (TBrC).

Received: September 22, 2014

Revised: December 11, 2014



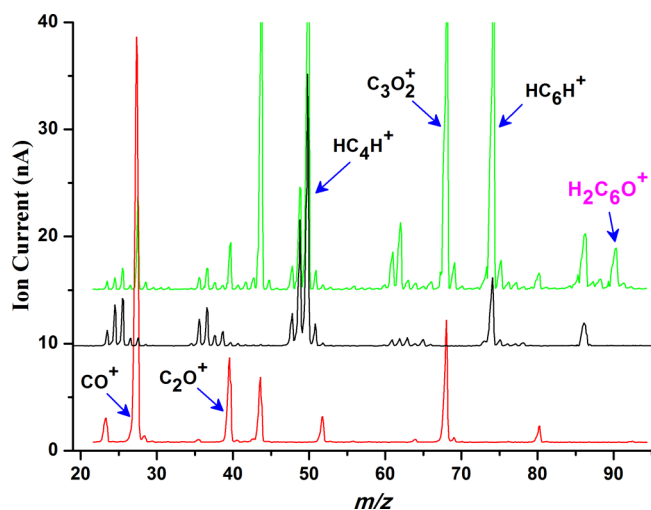


**Figure 1.** Mass spectra of  $\text{C}_3\text{O}_2$  (red),  $\text{HC}_4\text{H}$  (black), and 1:1 mixture of  $\text{C}_3\text{O}_2$  and  $\text{HC}_4\text{H}$  (green). The  $\text{H}_2\text{C}_6\text{O}^+$  ( $m/z = 90$ ) peak appeared upon mixing  $\text{C}_3\text{O}_2$  and  $\text{HC}_4\text{H}$ .

**2.2. Matrix Isolation Spectroscopy.** The method used combines mass selection with matrix isolation spectroscopy.<sup>25</sup> Ions produced in the source are extracted by electrostatic lenses and then deflected  $90^\circ$  to eliminate neutrals. The  $m/z = 90$  cations are selected in a quadrupole mass filter and subsequently codeposited with neon (containing trace of chloromethane in a ratio 1:20 000) on a sapphire plate coated with rhodium held at 6 K.  $\text{CH}_3\text{Cl}$  captures free electrons emitted from metal surfaces by the impact of ions, diminishing the neutralization of cations and reducing the space charge.  $\text{CH}_3\text{Cl}$  breaks into  $\text{CH}_3^\bullet$  and  $\text{Cl}^-$  by dissociative electron attachment, but these species do not interfere with the

absorption measurements in the visible and ultraviolet regions. Ions were also deposited in neon without  $\text{CH}_3\text{Cl}$  to obtain a higher concentration of neutrals. The growth of the matrix to 100–150  $\mu\text{m}$  thickness is controlled by observing light transmittance.

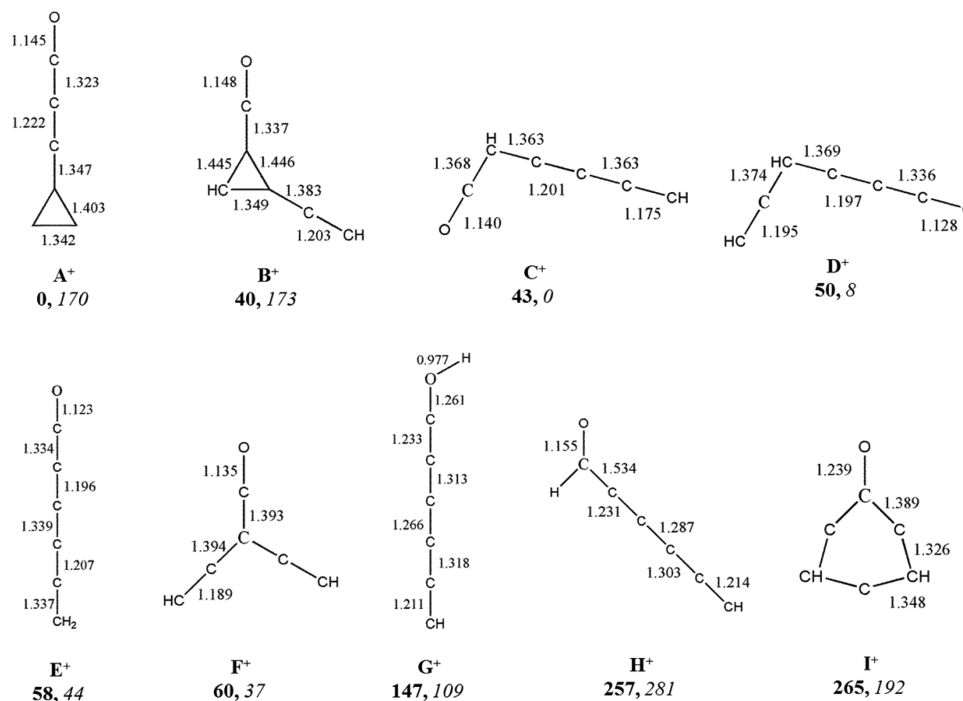
Spectra were recorded in the 250–1100 nm range by 60 nm overlapping sections. Halogen and high pressure xenon arc lamps were used as sources, and light after traveling through the 20 mm length of matrix was collected by optical fibers and transferred to the entrance slit of the spectrograph, wavelength dispersed, and recorded by CCD cameras.

### 3. COMPUTATION

Several structures (shown in Chart 1) can be expected for  $\text{H}_2\text{C}_6\text{O}^+$  formed via ion–molecule reactions between  $\text{C}_2\text{O}$  and  $\text{HC}_4\text{H}^+$ ,  $\text{C}_2\text{O}^+/\text{HC}_4\text{H}$ , or fragmentation of  $\text{TBrC}$ . The ground state geometries of nine plausible structures ( $\text{A}^+ - \text{I}^+$ ) were optimized using the MP2 method with the cc-pVTZ basis set with the Gaussian 09 program.<sup>26</sup> The ground state vibrations were calculated for each molecule to find real minima. The most stable isomer  $\text{A}^+$ ;  $\text{B}^+$ ,  $\text{C}^+$ ,  $\text{D}^+$ ,  $\text{E}^+$ , and  $\text{F}^+$  lie 40–60 kJ/mol and  $\text{G}^+$ ,  $\text{H}^+$ , and  $\text{I}^+$  140–265 kJ/mol to higher energy. Among the neutral counterparts, structure **C** is the global minimum and **D** is less stable by 8 kJ/mol.

The equilibrium coordinates obtained from the MP2 method were refined with the second order multiconfigurational perturbation theory (CASPT2) implemented in the Molcas software.<sup>27,28</sup> The CASPT2 calculations to obtain the ground state geometries of the  $\text{H}_2\text{C}_6\text{O}^+$  isomers were carried with the 9/9 active space. These coordinates were used for the prediction of vertical electronic excitation energies. The calculations with a larger active space (11/11) used the multistate (MS) CASPT2 option, with wave functions

**Chart 1.** Structures and Relative Ground State Energies (kJ mol<sup>−1</sup>) of  $\text{H}_2\text{C}_6\text{O}^+$  Cations (Bold Numbers) and Neutrals (Italic Numbers), Calculated with the MP2 Method and cc-pVTZ Basis Set<sup>a</sup>



<sup>a</sup>Bond lengths (Å) correspond to the optimized cation geometries.

optimized for the average energy of eight roots. Vertical excitation energies of **B** and **F** were also obtained at the MS-CASPT2 level with a 12/12 active space.

#### 4. RESULTS AND DISCUSSION

Moderately intense absorptions are detected in the 320–530 nm region (Figure 2, upper traces) after trapping in neon mass

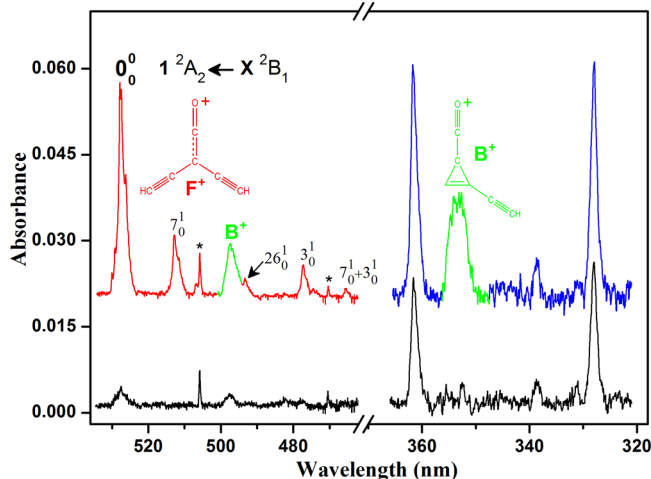


**Figure 2.** Electronic absorption spectra recorded after deposition of  $\text{H}_2\text{C}_6\text{O}^+$  produced from a 1:1 mixture of  $\text{C}_3\text{O}_2$  and diacetylene (upper traces) and after 20 min irradiation with  $\lambda > 260$  nm photons (lower traces). Bands denoted by asterisks (\*) belong to  $\text{C}_2^+$ .

selected  $\text{H}_2\text{C}_6\text{O}^+$  produced from a 1:1 mixture of  $\text{C}_3\text{O}_2$  and diacetylene. Two groups of bands, which differ in width, are apparent in the spectrum. The narrower features start around 528, 362, and 329 nm and broader ones start at  $\sim 497$  and  $\sim 354$  nm. The 362 and 329 nm absorptions are  $2^2\Pi_g \leftarrow X^2\Pi_u$  and  $3^2\Pi_g \leftarrow X^2\Pi_u$  transitions of  $l\text{-HC}_5\text{H}^+$ .<sup>29</sup> These have been measured in an earlier study and are shown in the red trace of Figure 3 with the absorptions detected after deposition of  $\text{H}_2\text{C}_6\text{O}^+$  in black. The traces were scaled to the intensity of the

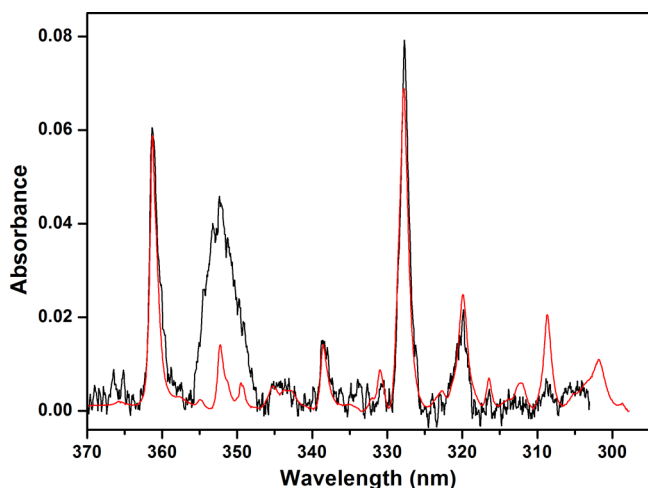


**Figure 3.** Electronic absorption spectra recorded after deposition of  $\text{H}_2\text{C}_6\text{O}^+$  generated from a 1:1 mixture of  $\text{C}_3\text{O}_2$  and diacetylene (black), and after deposition of  $\text{HC}_5\text{H}^+$  produced from diacetylene (red). The spectrum of  $\text{HC}_5\text{H}^+$  is normalized to the intensity of the 362 nm band.

362 nm band. The  $\text{HC}_5\text{H}^+$  cation is produced in the matrix as a result of collisionally induced fragmentation of  $\text{H}_2\text{C}_6\text{O}^+$  during deposition.

The matrix was exposed for 20 min to UV light ( $\lambda > 260$  nm), resulting in the detachment of electrons from  $\text{Cl}^-$  and neutralization of cations. The spectrum obtained is shown as the lower traces in Figure 2. The absorptions starting at 528, 497, and 354 nm almost disappeared, whereas the ones of  $\text{HC}_5\text{H}^+$  reduced. The  $\text{HC}_5\text{H}^+$  bands behave in a regular way under UV irradiation—their intensity decreases because of neutralization—whereas for the new absorptions additional decay channels are open: isomerization and/or fragmentation. No new peaks appeared after UV irradiation.  $\text{H}_2\text{C}_6\text{O}^+$  ions were also deposited in a pure neon matrix, but only a weak absorption at 528 nm was detected. Deposition of ions without the  $\text{CH}_3\text{Cl}$  scavenger favors trapping of neutral counterparts because of electron availability in the matrix. The behavior of the absorption features in Figure 2 under exposure to UV light indicates that they belong to photounstable isomer(s) of  $\text{H}_2\text{C}_6\text{O}^+$ . Because the neutral counterparts of  $\text{H}_2\text{C}_6\text{O}^+$  were not observed after photobleaching, or in pure neon, they do not have electronic transitions in the 250–1100 nm detection range, or these are weak.

The excitation energies of the neutral counterparts of the observed cations were calculated with MS-CASPT2 to explain why their absorptions were not observed. The results are collected in Table S11 in the Supporting Information. As can be seen, the strongest transitions fall in the UV range beyond the experimental detection range.

$\text{H}_2\text{C}_6\text{O}^+$  was also produced from TBrC and deposited. The spectrum obtained consists of two broader features starting at 497 and 354 nm and a weak absorption at 528 nm (Figure 4,

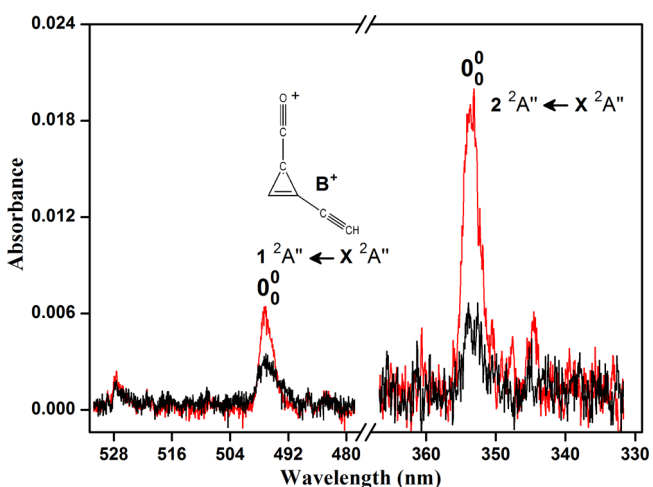


**Figure 4.** Electronic absorption spectra of  $\text{H}_2\text{C}_6\text{O}^+$  obtained after deposition of  $m/z = 90$  ions produced from 2,4,4,6-tetrabromo-2,5-cyclohexadienone (red) and after 20 min irradiation with 250–390 nm photons (black).

red trace). After irradiation (260–390 nm) the 497 and 354 nm absorptions diminish substantially, implying that they belong to the same  $\text{H}_2\text{C}_6\text{O}^+$  isomer. The decay of the absorptions under such irradiation conditions is due to photoinstability of the cation, because neutralization is not efficient at these wavelengths.

Use of different precursors for the production of  $\text{H}_2\text{C}_6\text{O}^+$  established that two isomers contribute to the spectra (Figures

2–4). One has a weak transition in the visible (2.49 eV; 497 nm) and a much stronger in the UV (3.51 eV; 354 nm). The second cation is characterized by the strong transition in the visible (2.35 eV; 528 nm) with resolved vibrational structure.

Vertical excitation energies of nine  $\text{H}_2\text{C}_6\text{O}^+$  isomers were calculated with MS-CASPT2 to assign the observed absorptions to specific species. The results for the likely candidates are collected in Table 1 and for the remaining ones in the

**Table 1. Excitation Energies ( $E_{\text{cal}}$ , eV) and Oscillator Strengths ( $f$ ) of  $\text{H}_2\text{C}_6\text{O}^+$  Isomers Calculated by the MS-CASPT2 Method and Comparison with the Observations ( $E_{\text{obs}}$ , eV)**

species	transition	$E_{\text{cal}}$	$f$	$E_{\text{obs}}$
$\text{B}^+$ ( $\text{C}_5$ )	$1^2\text{A}'' \leftarrow \text{X}^2\text{A}''$	2.68	0.024	2.49
	$2^2\text{A}'' \leftarrow \text{X}^2\text{A}''$	3.68	0.200	3.51
	$3^2\text{A}'' \leftarrow \text{X}^2\text{A}''$	5.32	0.100	
	$4^2\text{A}'' \leftarrow \text{X}^2\text{A}''$	5.73	0.060	
$\text{D}^+$ ( $\text{C}_5$ )	$1^2\text{A}'' \leftarrow \text{X}^2\text{A}''$	2.60	0.040	
	$2^2\text{A}'' \leftarrow \text{X}^2\text{A}''$	3.67	0.49	
	$3^2\text{A}'' \leftarrow \text{X}^2\text{A}''$	4.16	0.0069	
	$4^2\text{A}'' \leftarrow \text{X}^2\text{A}''$	4.44	0.0044	
$\text{F}^+$ ( $\text{C}_{2v}$ )	$5^2\text{A}'' \leftarrow \text{X}^2\text{A}''$	4.70	0.015	
	$1^2\text{A}_2 \leftarrow \text{X}^2\text{B}_1$	2.38	0.11	2.35
	$2^2\text{A}_2 \leftarrow \text{X}^2\text{B}_1$	5.58	0.051	
	$1^2\text{B}_1 \leftarrow \text{X}^2\text{B}_1$	4.26	0.007	
$\text{C}^+$ ( $\text{C}_5$ )	$2^2\text{B}_1 \leftarrow \text{X}^2\text{B}_1$	5.30	0.27	
	$2^2\text{B}_1 \leftarrow \text{X}^2\text{B}_1$	5.90	0.005	
	$1^2\text{A}'' \leftarrow \text{X}^2\text{A}''$	2.51	0.19	
	$2^2\text{A}'' \leftarrow \text{X}^2\text{A}''$	3.92	0.17	
	$3^2\text{A}'' \leftarrow \text{X}^2\text{A}''$	4.08	0.030	
	$4^2\text{A}'' \leftarrow \text{X}^2\text{A}''$	4.47	0.15	

Supporting Information, Table SI2. Among these only structures  $\text{B}^+$  and  $\text{D}^+$  can be responsible for the two absorptions at 497 and 354 nm. The calculations predict a moderately intense transition with energy 2.68 ( $f = 0.024$ ) and 2.60 eV ( $f = 0.040$ ) and about a 10 times stronger transition at 3.68 and 3.67 eV for  $\text{B}^+$  and  $\text{D}^+$ , respectively. The oscillator strengths are in accord with the intensities of the 497 and 354 nm systems. The vertical excitation energies overestimate the onsets of the observed systems by  $\sim 0.2$  eV; calculated adiabatic values should match better with the experimental ones. As  $\text{D}^+$  lies only slightly higher in energy than  $\text{B}^+$ , it cannot be eliminated from consideration as the carrier.

In contrast to isomers  $\text{B}^+$  and  $\text{D}^+$ , for which the spectroscopic signatures are the two electronic systems in the visible and UV, the carrier of the 528 nm system should possess only a single strong transition around 2.35 eV. Apart from isomers  $\text{B}^+$  and  $\text{D}^+$  four others— $\text{C}^+$ ,  $\text{E}^+$ ,  $\text{F}^+$ , and  $\text{G}^+$ —have transitions in this region. The first electronic system of  $\text{E}^+$  at 2.45 eV is weak ( $f = 0.006$ ) and two stronger ones ( $f = 0.02$  and  $0.065$ ) are predicted in the 3.1–3.3 eV range, in contrast to the observation. The first electronic transition of  $\text{G}^+$  is calculated at 2.26 eV with  $f = 0.085$ , the next one is calculated at 3.22 eV ( $f = 0.045$ ), but it can be excluded as the carrier because its UV transition should also be detectable. Isomer  $\text{C}^+$  is also eliminated from consideration: although the  $1^2\text{A}'' \leftarrow \text{X}^2\text{A}''$  electronic transition at 2.51 eV is very strong ( $f = 0.2$ ), an equally intense band at 3.92 eV is predicted, in contrast to the observation.

Isomer  $\text{F}^+$  fulfills the criteria for the carrier of 528 nm system: a strong transition at 2.38 eV ( $f = 0.11$ ) close to the observation (2.35 eV) and a nondetectable absorption in the UV. The next strongest transition of  $\text{F}^+$  is predicted at 5.58 eV ( $f = 0.055$ ), beyond the experimental detection range. Moreover,  $\text{F}^+$  during deposition with  $\sim 50$  eV kinetic energy on solid neon can fragment to produce  $1\text{-HC}_5\text{H}^+$  and CO. The absorptions of  $1\text{-HC}_5\text{H}^+$  are detected (Figure 2). Therefore, the 528 nm system is assigned to the  $1^2\text{A}_2 \leftarrow \text{X}^2\text{B}_1$  transition of  $\text{F}^+$ . A well-resolved vibrational structure is apparent in the spectrum and results from the excitation of the  $\nu_7$ ,  $\nu_6$ , and  $\nu_3$  vibrational modes and their combinations. The assignment is based on the harmonic frequencies calculated for the ground state of  $\text{F}^+$  with the density functional theory (DFT) method using the B3LYP functional and cc-pVTZ basis set (see Table 2).

**Table 2. Absorption Band Maxima ( $\pm 0.1$  nm) of Electronic Transitions of  $\text{H}_2\text{C}_6\text{O}^+$  Isomers  $\text{B}^+$  and  $\text{F}^+$  in 6 K Neon Matrixes and Assignment Based on MS-CASPT2 Calculations<sup>a</sup>**

species	$\lambda$ (nm)	$\nu$ ( $\text{cm}^{-1}$ )	$\Delta\nu$ ( $\text{cm}^{-1}$ )	assignment	transition
$\text{F}^+$	527.6	18 954	0	$0_0^0$	$1^2\text{B}_1 \leftarrow \text{X}^2\text{A}_2$
	512.8	19 501	547	$\nu_7$	
	493.1	20 280	1326	$2\nu_6$	
	476.9	20 969	2015	$\nu_3$	
	465.0	21 505	2551	$\nu_3 + \nu_7$	
$\text{B}^+$	497.3	20 109	0	$0_0^0$	$1^2\text{A}'' \leftarrow \text{X}^2\text{A}''$
	353.6	28 281	0	$0_0^0$	$2^2\text{A}'' \leftarrow \text{X}^2\text{A}''$

<sup>a</sup>The vibrational interpretation of the  $\text{F}^+$  spectrum is based on the calculated ground state harmonic frequencies. Totally symmetric vibrations ( $\text{cm}^{-1}$ ) of  $\text{F}^+$  calculated with DFT using the B3LYP functional and the cc-pVTZ basis set for  $\nu_1$ – $\nu_7$  were 3412, 2276, 2169, 1198, 754, 669, 543, and 121.

The reactants which lead to the formation of  $\text{H}_2\text{C}_6\text{O}^+$  are  $\text{C}_2\text{O}$  and  $\text{HC}_4\text{H}^+$ , and/or  $\text{C}_2\text{O}^+$  with  $\text{HC}_4\text{H}$ , as both cations were observed in the mass spectrum of the precursor. The ionization potential (IP) of diacetylene is 10.17 eV,<sup>30</sup> but the experimental value for  $\text{C}_2\text{O}$  is unknown. Therefore, the IPs of  $\text{HC}_4\text{H}$  and  $\text{C}_2\text{O}$  were calculated using the CCSD(T) method for the geometry optimized at the CCSD level, leading to 10.08 eV for  $\text{HC}_4\text{H}$  and 10.81 eV for  $\text{C}_2\text{O}$ . Hence, the most probable way of  $\text{H}_2\text{C}_6\text{O}^+$  production is the reaction of  $\text{C}_2\text{O}$  with  $\text{HC}_4\text{H}^+$ . The reactions of  $\text{C}_2\text{O}^+$  with diacetylene, as well as  $\text{C}_2\text{O}$  with  $\text{HC}_4\text{H}^+$ , are exothermic. The calculated enthalpy of the reaction between  $\text{C}_2\text{O}$  and  $\text{HC}_4\text{H}^+$  is 539 kJ/mol at the MP2/cc-pVTZ level of theory.  $\text{C}_2\text{O}$  in the  $^3\Sigma^-$  ground state is a reactive biradical with two electrons on the terminal carbon atom.  $\text{C}_2\text{O}$  attacks the electrophilic center of  $\text{HC}_4\text{H}^+$ , which is located on the middle carbon atoms (Supporting Information, Table SI3).

In the case of the reaction  $\text{C}_2\text{O}^+$  with  $\text{HC}_4\text{H}$ , a charge exchange is likely the first step.  $\text{C}_2\text{O}^+$  in the  $^2\Pi$  ground state possesses an unpaired electron on the terminal carbon atom and reacts as a radical. The preferred site of reaction of  $\text{C}_2\text{O}^+$  with diacetylene is on the electronegative carbon atom adjacent to the hydrogen atoms (Supporting Information, Table SI3).

On the basis of the calculated vertical excitation energies and the oscillator strengths (Table 1) as well as the ground state stabilities (Chart 1) of  $\text{B}^+$  and  $\text{D}^+$ , one cannot firmly deduce the carrier for the 497 and 354 nm absorptions. However, the structure of  $\text{B}^+$  produced via dissociative ionization of  $\text{TBrc}$  is



analogous to that of the  $C_6H_4^+$  isomer: three-carbon-member ring with aliphatic chain ( $T^+$ ) generated from 1,2-dibromobenzene under similar discharge conditions.<sup>31</sup> MS-CASPT2 calculation predicts a strong electronic transition ( $f = 0.2$ ) at 4.45 eV (280 nm) for neutral  $D$  which was not observed (see Supporting Information, Table S11). Thus, the 497 and 354 nm systems are assigned to the  $1^2A'' \leftarrow X^2A''$  and  $2^2A'' \leftarrow X^2A''$  electronic transitions of  $B^+$ .

## 5. CONCLUSIONS

Two isomers of  $H_2C_6O^+$  (2-ethynylcycloallyl)methanone cation,  $B^+$ , and 2-ethynylbut-3-yn-1-enone-1-ylide,  $F^+$ , were produced in a hot cathode discharge source from a mixture of carbon suboxide and diacetylene. The reactions between  $C_2O$  and  $HC_4H^+$ , or  $C_2O^+$  and  $HC_4H$ , are exothermic. They should be considered in the astrophysical models as a way of incorporation of oxygen into the hydrocarbon moieties. Three absorption systems starting at 528, 497, and 354 nm are detected following deposition of  $H_2C_6O^+$  in a 6 K neon matrix. These are assigned to the  $1^2A_2 \leftarrow X^2B_1$  electronic transition of  $F^+$ , and  $1^2A'' \leftarrow X^2A''$  and  $2^2A'' \leftarrow X^2A''$  of  $B^+$ , on the basis of mass selection, the cationic nature, and the calculated excitation energies with the CASPT2 method. The  $B^+$  and  $F^+$  isomers were found unstable under 260–390 nm photon exposure. Oxygenated hydrocarbons and their ions, such as  $H_2C_6O^+$ , are likely reactive intermediates in combustion, and the present spectroscopic data provide the means to monitor them in situ via their electronic absorptions and can serve as a starting point for the gas phase study.

## ■ ASSOCIATED CONTENT

### ● Supporting Information

Tables contain calculated excitation energies of five cation and three neutral isomers, Mulliken charges and spin densities of  $HC_4H/HC_4H^+$  and  $C_2O/C_2O^+$ . This material is available free of charge via the Internet at <http://pubs.acs.org>.

## ■ AUTHOR INFORMATION

### Corresponding Author

\*E-mail: [j.p.maier@unibas.ch](mailto:j.p.maier@unibas.ch). Tel.: +41 612673826. Fax: +41 612673855.

### Notes

The authors declare no competing financial interest.

## ■ ACKNOWLEDGMENTS

This work was supported by the Swiss National Science Foundation (Project 200020-124349/1).

## ■ REFERENCES

- (1) Cameron, A. G. W. Abundances of the Elements in the Solar System. *Space Sci. Rev.* **1973**, *15*, 121–146.
- (2) Snow, T. P.; Bierbaum, V. M. Ion Chemistry in the Interstellar Medium. *Annu. Rev. Anal. Chem.* **2008**, *1*, 229–259.
- (3) Thaddeus, P.; McCarthy, M. C. Carbon Chains and Rings in the Laboratory and in Space. *Spectrochim. Acta, Part A* **2001**, *57*, 757–774.
- (4) Lee, J.-E.; Evans, N. J.; Shirley, Y. L. Chemistry and Dynamics in Pre-Protostellar Cores. *Astrophys. J.* **2013**, *583*, 789–808.
- (5) Solomon, P.; Jefferts, K. B.; Penzias, A. A.; Wilson, R. W. Observation of CO Emission at 2.6 Millimeters from IRC+10216. *Astrophys. J.* **1971**, *163*, L53–L56.
- (6) Smith, A. M.; Stecher, T. P. Carbon Monoxide in the Interstellar Spectrum of Zeta Ophiuchi. *Astrophys. J.* **1971**, *164*, L43–L47.

- (7) Dickinson, D. F. Detection of Silicon Monoxide at 87 GHz. *Astrophys. J.* **1972**, *175*, L43–L46.
- (8) Tenenbaum, E. D.; Woolf, N. J.; Ziurys, L. M. Identification of Phosphorus Monoxide ( $X^2\Pi_r$ ) in VY Canis Majoris: Detection of the First P–O Bond in Space. *Astron. Astrophys.* **2007**, *666*, L29–L32.
- (9) Tenenbaum, E. D.; Ziurys, L. M. Millimeter Detection of AlO ( $X^2\Sigma^+$ ): Metal Oxide Chemistry in the Envelope of VY Canis Majoris. *Astrophys. J.* **2009**, *694*, L59–L63.
- (10) Hillenbrand, L. A.; Knapp, G. R.; Padgett, D. L.; Rebull, L. M.; McGehee, P. M. Optical TiO and VO Band Emission in Two Embedded Protostars: IRAS 04369 + 2539 and IRAS 05451 + 0037. *Astron. J.* **2012**, *143*, 1–13.
- (11) Hollis, J. M.; Remijan, A. J.; Jewell, P. R.; Lovas, F. J. Cyclopropenone ( $C_3H_2O$ ): A New Interstellar Ring Molecule. *Astrophys. J.* **2006**, *642*, 933–939.
- (12) Cordiner, M. A.; Charnley, S. B. Gas-Grain Models for Interstellar Anion Chemistry. *Astrophys. J.* **2012**, *749*, 120 (1–10).
- (13) Adams, N. G.; Smith, D.; Giles, K.; Herbst, E. The Production of  $C_nO$ ,  $HC_nO$  and  $H_2C_nO$  Molecules in Dense Interstellar Clouds. *Astron. Astrophys.* **1989**, *220*, 269–271.
- (14) Klemperer, W. Carrier of the Interstellar 89.190 GHz Line. *Nature* **1970**, *227*, 1230.
- (15) Thaddeus, P.; Guelin, M.; Linke, R. A. Three New ‘Nonterrestrial’ Molecules. *Astrophys. J.* **1981**, *246*, L41–L45.
- (16) Mihn, Y. C.; Irvine, W. M.; Ziurys, L. M. Observations of Interstellar  $HOCO^+$ —Abundance Enhancements toward the Galactic Center. *Astrophys. J.* **1988**, *334*, 175–181.
- (17) Ohishi, M.; Ishikawa, S.-I.; Amano, T.; Oka, H.; Irvine, W. M.; Dickens, J. E.; Ziurys, L. M.; Apponi, A. J. Detection of A New Interstellar Molecular Ion,  $H_2COH^+$  (Protonated Formaldehyde). *Astrophys. J.* **1996**, *471*, L61–L64.
- (18) Blake, G. A.; Sastry, K. V. L. N.; De Lucia, F. C. The Laboratory Millimeter and Submillimeter Spectrum of  $HCO$ . *J. Chem. Phys.* **1984**, *80*, 95–101.
- (19) Endo, Y.; Hirota, E. The Submillimeter-Wave Spectrum of the HCCO Radical. *J. Chem. Phys.* **1987**, *86*, 4319–4326.
- (20) Cooksy, A. L.; Watson, J. K. G.; Gottlieb, C. A.; Thaddeus, P. The Structure of the HCCCO Radical. Rotational Spectra and Hyperfine Structure of Monosubstituted Isotopomers. *J. Chem. Phys.* **1994**, *101*, 178–186.
- (21) Kohguchi, H.; Ohshima, Y.; Endo, Y. Pulsed-Discharge Nozzle Fourier-Transform Microwave Spectroscopy of the  $HC_4O$  Radical. *J. Chem. Phys.* **1994**, *101*, 6463–6469.
- (22) Mohamed, S.; McCarthy, M. C.; Cooksy, A. L.; Hinton, C.; Thaddeus, P. Rotational Spectra of the Carbon-Chain Radicals  $HC_5O$ ,  $HC_6O$  and  $HC_7O$ . *J. Chem. Phys.* **2005**, *123*, 234301 (1–8).
- (23) Strelnikov, D.; Reusch, R.; Krätschmer, W. Oxides of Long Carbon Chains: Results Obtained on IR and UV–Vis Absorptions. *J. Mol. Spectrosc.* **2007**, *243*, 189–193.
- (24) Joseph, S. M. E.; Fulara, J.; Garkusha, I.; Maier, J. P. Electronic Absorption Spectra of  $C_7O$  and  $C_7O^+$  in 6 K Neon Matrices. *Mol. Phys.* **2013**, *111*, 1977–1982.
- (25) Nagy, A.; Garkusha, I.; Fulara, J.; Maier, J. P. Electronic Spectroscopy of Transient Species in Solid Neon: The Indene Motif Polycyclic Hydrocarbon Cation Family  $C_9H_y^+$  ( $y=7-9$ ) and their Neutrals. *Phys. Chem. Chem. Phys.* **2013**, *15*, 19091–19101.
- (26) Frisch, M. J.; Trucks, G. W.; Schlegel, H. B.; Scuseria, G. E.; Robb, M. A.; Cheeseman, J. R.; Scalmani, G.; Barone, V.; Mennucci, B.; Petersson, G. A.; et al. *Gaussian 09*, revision D.01; Gaussian, Inc.: Wallingford, CT, 2009.
- (27) Andersson, K.; Malmqvist, P.-A.; Roos, B. O.; Sadlej, A. J.; Wolinski, K. Second-Order Perturbation Theory with a CASSCF Reference Function. *J. Phys. Chem.* **1990**, *94*, 5483–5488.
- (28) Andersson, K.; Malmqvist, P.-A.; Roos, B. O. Second-Order Perturbation Theory with a Complete Active Space Self-Consistent Field Reference Function. *J. Chem. Phys.* **1992**, *96*, 1218–1226.
- (29) Fulara, J.; Nagy, A.; Garkusha, I.; Maier, J. P. Higher Energy Electronic Transitions of  $HC_{2n+1}H^+$  ( $n=2-7$ ) and  $HC_{2n+1}H$  ( $n=4-7$ ) in Neon Matrices. *J. Chem. Phys.* **2010**, *133*, 024304 (1–9).

(30) Bieri, G.; Schmelzer, A.; Asbrink, L.; Jonsson, M. Fluorine and the Fluoroderivatives of Acetylene and Diacetylene Studied by 30.4 nm He(II) Photoelectron Spectroscopy. *Chem. Phys.* **1980**, *49*, 213–224.

(31) Fulara, J.; Nagy, A.; Filipkowski, K.; Thimmakondur, V. S.; Stanton, J. F.; Maier, J. P. Electronic Transitions of  $C_6H_4^+$  Isomers: Neon Matrix and Theoretical Studies. *J. Phys. Chem. A* **2013**, *117*, 13605–13615.